Solid Earth Discuss., doi:10.5194/se-2016-152, 2016
Manuscript under review for journal Solid Earth
Published: 9 December 2016

Solid Earth Discussions
Open Access
EGU

Soil Atterberg limits of different weathering profiles of the collapsing gullies in the hilly granitic region of south China

Yusong Deng [1], Chongfa Cai [1]*, Dong Xia [2], Shuwen Ding [1], Jiazhou Chen [1]

[1]*Key Laboratory of Arable Land Conservation (Middle and Lower Reaches of Yangtze River) of the Ministry of Agriculture, College of Resources and Environment, Huazhong Agricultural University, Wuhan, 430070, People's Republic of China*

[2] *College of hydraulic and Environmental engineering, China Three Gorges University, Yichang 443002, China*

*Corresponding author. E-mail: chongfacai@126.com

Post address:

College of Resources and Environment, Huazhong Agricultural University, Wuhan 430070, China.

Tel: +86-27-87288249

Fax: +86-27-87288249

Other co-authors' e-mails: dennyus@163.com (Yusong Deng)

xiadongsanxia@163.com (Dong Xia)

dingshuwen@mail.hzau.edu.cn (Shuwen Ding)

jzchen@mail.hzau.edu.cn (Jiazhou Chen)

Solid Earth Discuss., doi:10.5194/se-2016-152, 2016
Manuscript under review for journal Solid Earth
Published: 9 December 2016

Abstract. Collapsing gully erosion is one of the most serious natural hazards in the hilly granitic region of south China. However, few studies have been performed on the relationship of soil Atterberg limits with soil profiles of the collapsing gullies. Soil Atterberg limits, which include plastic limit and liquid limit, have been proposed as indicators for soil vulnerability to degradation. Here, the soil Atterberg limits within different weathering profiles and their relationships with soil physico-chemical properties were investigated by characterizing four collapsing gullies in four counties (Tongcheng County, Gan County, Anxi County and Wuhua County, labeled as TC, GX, AX and WH, respectively) in the hilly granitic region of southern China. The results showed that with the fall of weathering degree (from surface layer to detritus layer), there was a sharp decrease in plastic limit, liquid limit, plasticity index, soil organic matter, cation exchange capacity and free iron oxide, a gradual increase in liquidity index, a sharp increase in particle density and bulk density followed by a slight decline, as well as a decrease in the finer soil particles (silt and clay), a noticeable decline in the clay contents, and a considerable increase in the gravel and sand contents. The plastic limit varied from 19.43 to 35.93 % in TC, 19.51 to 33.82 % in GX, 19.32 to 35.58 % in AX and 18.91 to 36.56 % in WH while the liquid limit varied from 30.91 to 62.68 % in TC, 30.89 to 57.70 % in GX, 32.48 to 65.71 % in AX and 30.77 to 62.70 % in WH, respectively. The soil Atterberg limits in the sandy soil layers and detritus layers were lower than those in the surface layers and red soil layers, leading to the loss of bottom soil layers, the collapse of upper soil layers and finally the occurrence of collapsing gully erosion. The regression equation showed that soil Atterberg limits had significant and positive correlation with SOM, clay content, CEC and Fe_d, significant and negative correlation with sand content and no obvious correlation with other properties. The results of this study revealed that soil Atterberg limits are an informative indicator to reflect the weathering degree of different weathering profiles of the collapsing gullies in the hilly granitic region.

1 Introduction

In 1911, Atterberg proposed the limits of consistency for agricultural purposes to get a clear concept of the range of water contents of a soil in the plastic state (Atterberg, 1911). These limits of consistency, namely plastic limit and liquid limit, are well known as soil Atterberg limits. Plastic

Solid Earth Discuss., doi:10.5194/se-2016-152, 2016
Manuscript under review for journal Solid Earth
Published: 9 December 2016

limit is the boundary between semi-solid and plastic state, and liquid limit separates plastic state from liquid state (Campbell, 2001). The methods developed by Casagrande (1932, 1958) to determine the liquid and plastic limits are considered as standard international tests. The width of the plastic state (liquid limit minus plastic limit), the plasticity index, is very useful for characterization, classification and prediction of the engineering behavior of fine soils. Moreover, some research attempts have been made on the relationship between in situ water content and Atterberg limits, the liquidity index, which is the ratio of the difference between the natural moisture content and the plastic limit to the plastic limit (Intan et al., 2014; Rashid et al., 2014). Atterberg limits were used in early studies on the tillage of soils, with the plastic limit recognized as the highest possible soil water content for cultivation (Baver, 1930; Jong et al., 1990). Later on, Atterberg limits were mainly used in the classification of soils for engineering purposes. They also provide information for interpreting several soil mechanical and physical properties such as shear strength, bearing capacity, compressibility and shrinkage-swelling potential (Archer, 1975; Wroth, 1978; Cathy et al., 2008; McBride, 2008). Meanwhile, Atterberg limits are also essential for infrastructure design (e.g., construction of buildings and roads) (Zolfaghari et al., 2015). These studies clearly show that there is a close relationship between Atterberg limits and certain properties of soils. More recently, Atterberg limits have been proposed as indicators for soil vulnerability to degradation processes of both natural and anthropogenic origin. Yalcin (2007) emphasized that, when subjected to water saturation, soils with limited cohesion are susceptible to erosion during heavy rainfall. Curtaz et al. (2014), Vacchiano et al. (2014) and Stanchi et al. (2012) provided a novel overview on plastic limit and liquid limit in common soil types and proposed plastic limit and liquid limit as indicators to assess the vulnerability of mountain soils to erosion.

Soil erosion is important problems in mountain areas as remarked by Douglas et al. (2011) and MorenoRamón et al. (2014), and may result in considerable soil degradation (Cerdà et al., 2007; Pavlova et al., 2014; Jordán et al., 2014; Peng et al., 2015; Muñoz-Rojas et al., 2016). Collapsing gully is a serious type of soil erosion widely distributed in the hilly granitic region of southern China, which is formed in the hill slopes covered by thick granite weathering mantle (Xu, 1996). Collapsing gully was first proposed by Zeng in 1960, which is a composite erosion formed by hydraulic scour and gravitational collapse (Zeng, 1960; Jiang et al., 2014; Xia et al., 2015; Deng et

Solid Earth Discuss., doi:10.5194/se-2016-152, 2016
Manuscript under review for journal Solid Earth
Published: 9 December 2016

al., 2016). These gullies develop quickly and erupt suddenly, with an annual average erosion of over 50 kt km^{-2} yr^{-1} in these areas, more than 50-fold faster than the erosion on gentler slopes or on slopes with high vegetation cover (Zhong et al., 2013). The flooding, debris flows, and other disasters resulting from collapsing gullies can jeopardize sustainable development in the related regions. From 1950 to 2005, gully erosion affected 1220 km^2 in the granitic red clay soil region, leading to the loss of more than 60 Mt of soil (Zhang, 2010). It is worth mentioning that the collapsing gullies in turn caused the loss of 360,000 ha of farmland, 521,000 houses, 36,000 km of road, 10,000 bridges, 9000 reservoirs, and 73,000 ponds, as well as an economic loss of 3.28 billion USD that affected 9.17 million residents (Jiang et al., 2014; Liang et al., 2009). According to a 2005 survey by the Monitoring Center of Soil and Water Conservation of China, collapsing gullies are widely distributed in the granitic red clay soil regions of south China, which includes Guangdong, Jiangxi, Hubei, Hunan, Fujian, Anhui, and Guangxi provinces. It is incredible that the number of collapsing gullies is up to 239, 100, posing a serious threat to the local people (Feng et al., 2009). A collapsing gully system consists of five parts: (1) upper catchment, where a large amount of water is accumulated; (2) collapsing wall, where mass soil wasting, water erosion and gravity erosion are quite serious; (3) colluvial deposit, where residual material is deposited; (4) scour channel, where the sediment accumulation and transport is usually significantly deep and narrow; (5) alluvial fan, the zone below the gully mouth where sediments transported by the collapse are deposited (Xu, 1996; Sheng and Liao, 1997; Xia et al., 2015) (Figure 1). Collapsing gully poses a serious problem for land utilization and development and the establishment of sustainable environmental solutions in southern China. Unfortunately, there is no effective approach to prevent such disasters currently, and this soil erosion has affected the lives of tens of millions of Chinese citizens (Gao et al., 2011).

In a collapsing gully system, slumps and massive collapses of the collapsing wall are one of the main influential factors causing the collapsing gully enlargement and development (Xia et al., 2015). Researchers have paid close attention to the damage of collapsing gully, and found that there is a close relationship among the stability of the collapsing wall, the erosion amount and the development speed (Xu, 1996; Sheng and Liao, 1997; Luk et al., 1997a, 1997b; Lan et al., 2003). Qiu (1994) pointed out that the mechanical composition of soil and the change of its action with

Solid Earth Discuss., doi:10.5194/se-2016-152, 2016
Manuscript under review for journal Solid Earth
Published: 9 December 2016

water have an important influence on the development of collapsing gully. Li (1992) stated that there is an important relationship between the soil water content and critical height of collapsing wall, with the critical height of the wall being 8-9 m when the water content is low, which is only 2-3 m in the saturated state. Zhang et al. (2013) pointed out that the granite soil is easy to disintegrate with increasing water content, and the process is irreversible. Zhang et al.(2012) proposed that the cohesion and internal friction angle of the soil showed a nonlinear attenuation trend with the increase of water content, and the shear strength index showed a peak value when the soil water content was about 13%. Liu et al. (2015) and Deng et al. (2015) reported that the water content of the collapsing wall gradually increased with the increase of the soil depth. Deng et al. (2016) proposed that the soil water characteristic curve of granite weathering layer is different, and the lower soil layers have greater dewatering ability than the upper soil layers. From these studies, we can find the soil water content is a common influencing factor, and the stability of the collapsing wall will vary with it. Wang et al. (2000) believe that the mechanical properties of soil will change significantly when the rain is in full contact with the soil. Similar conclusions were reported by Luk et al. (1997a) who revealed the main cause for collapse occurrence is the short-term rainfall intensity. The liquid limit and plastic limit of soil, namely the soil Atterberg limits, are its highest and lowest water content in the plastic state, which are of important significance in predicting the influence of surface runoff and rainfall on the collapsing gully. In recent years, few studies have been performed on the relationship between Atterberg limits and soil profiles in the hilly granitic region of southern China.

In this paper, we selected four collapsing gullies in the four counties located in a different latitude of South China to analyze the influence factors for collapsing gully and the relationships between soil Atterberg limits and soil physico-chemical properties. The objectives of this study are: 1) to evaluate the similarities and differences in soil Atterberg limits and soil physico-chemical properties of different weathering profiles among the four collapsing gullies; 2) to investigate the relationship between soil Atterberg limits and soil physico-chemical properties by analyzing the status and variation of soil Atterberg limits and 3) to explore the possibility of using soil Atterberg limits as an integrated index for quantifying collapsing gully and soil weathering degree of different weathering profiles in the hilly granitic region.

Solid Earth Discuss., doi:10.5194/se-2016-152, 2016
Manuscript under review for journal Solid Earth
Published: 9 December 2016

145 *Insert*: Figure 1.

146 2 **Materials and methods**

147 **2.1 Study area**

148 The sampling plots(22°58′-29°24′N,110°51′-118°17′) are located in the hilly granitic region
149 of South China, including Tongcheng county in Hubei province, Gan county in Jiangxi province,
150 Anxi county in Fujian province, Wuhua county in Guangdong province and Cangwu county in
151 Guangxi province, which are the most serious collapsing gully erosion centers in South China and
152 thus were selected as the study sites. These study areas are in a temperate monsoonal continental
153 climate zone, with an average temperature of 15-22℃, an average annual precipitation of about
154 1500 mm with high variability. The region is dominated by the granite red soil (Humic Acrisols)
155 and developed in the Yanshan period. The soil erosion is serious in this region, especially the huge
156 amount of collapsing gullies. There were 1102, 4138, 4744, 22117 and 1592 collapsing gullies in
157 the Tongcheng county, Gan county, Anxi county, Wuhua county and Cangwu county, respectively.

158 **2.2 Soil sampling**

159 According to previous studies and the soil color and soil structural characteristics, the weathering
160 profiles of the collapsing gullies of the study area in the hilly granitic region can be subdivided into
161 four soil layers: surface layer, red soil layer, sandy soil layer, detritus layer (Luk et al., 1997a; Zhang
162 et al., 2012; Xia et al., 2015). Each soil layers have some common characteristics as reported by
163 Luk et al. (1997a).

164 This study focused on the development of four collapsing gullies in the south of China, including
165 Tongcheng county (TC), Gan county (GX), Anxi county (AX) and Wuhua county (WH), where the
166 development of collapsing gullies is concentrated. The soil samples were collected in surface layer,
167 red soil layer, sandy soil layer, detritus layer. According to the height of the collapsing gully wall,
168 we collected 6, 8, 8 and 8 soil samples in four weathered layers, respectively. The detritus layer of
169 the collapsing gully in Tongcheng County was not exposed, so the soil samples were not collected.
170 Descriptions of soil sample site and soil sampling depth are given in Tables 1 and 2.

171 When collecting the samples of each soil layer, about 1-2 kg soil sample was obtained by means
172 of quartering and transported to the laboratory for measurement of soil Atterberg limits (including
173 plastic limit and liquid limit) and soil physico-chemical properties (including soil particle density,

Solid Earth Discuss., doi:10.5194/se-2016-152, 2016
Manuscript under review for journal Solid Earth
Published: 9 December 2016

organic matter, cation exchange capacity and free iron oxide). At each layer, six soil samples were obtained by using cutting ring to determine soil bulk density and calculate the total porosity.

2.3 Soil analysis

The soil samples were air-dried and then sieved at the fraction <0.452 mm for Atterberg limits determination, and at <2mm for measurement of soil physical and chemical properties including particle density, particle-size distribution and chemical analyses. Soil Atterberg limits (liquid limit, and plastic limit) were determined using the air-dried soil for each layer according to the standard methods reported in S.I.S.S (1997) after ASTM D 4318-10e1 (2010), i.e. (Stanchi et al., 2015). The plasticity index and the liquidity index are obtained by the following Eq (1, 2).

$$\text{Plasticity index} = \text{liquid limit} - \text{plastic limit} \quad (1)$$

$$\text{Liquidity index} = (WC_{insitu} - \text{plastic limit}) / (\text{liquid limit} - \text{plastic limit}) \quad (2)$$

where WC_{insitu} is in situ water content.

The particle density (PD) was measured by the pycnometer method, the bulk density (BD) was determined by the cutting ring method, and the total porosity (TP) was calculated as TP = 1 - (BD / PD) (Anderson and Ingram, 1993; Cerdà and Doerr, 2010). The particle-size distribution (PSD) was determined by the sieve and pipette method (Gee and Bauder, 1986). Soil organic matter (SOM) was measured by the $K_2Cr_2O_7$-H_2SO_4 oxidation method of Walkey-Black (Nelson and Sommers, 1982; Armo et al., 2014). Cation exchange capacity (CEC) was measured after extraction with ammonium acetate (Rhoades, 1982); Free iron oxide (Fed) were extracted by dithionite-citrate-bicarbonate (DCB) (Mehra and Jackson, 1958).

2.4 Statistical analysis

Statistical analyses were performed by SPSS 19.0 software (SPSS Inc., Chicago, IL, USA). A one-way analysis of variance (ANOVA) was performed to examine the effects of soil depth on soil Atterberg limits and soil physico-chemical properties. The least square difference (LSD) test (at $P<0.05$) was used to compare means of soil variables when the results of ANOVA were significant at $P<0.05$. Regression analysis was used to analyze the relationship between soil Atterberg limits and soil physico-chemical properties.

3 Results and discussion

3.1 Soil physico-chemical properties

Solid Earth Discuss., doi:10.5194/se-2016-152, 2016
Manuscript under review for journal Solid Earth
Published: 9 December 2016

The soil physical and chemical properties for the different weathering profiles in the four collapsing gullies (TC, GX, AX and WH) were described in terms of soil particle density (PD), soil bulk density (BD), total porosity (TP), soil organic matter (SOM), cation exchange capacity (CEC), free iron oxide (Fe_d) and particle size distribution (PSD). The values for these properties are shown in Table 2 and Table 3. Average values at varying soil layers including surface soil layer, red soil layer, sandy soil layer and detritus layer are given in Figure 2 and Figure 3.

3.1.1 Soil particle density (PD)

From Table 2, it can be seen that the soil PD was the highest in TC3 (2.68 g cm^{-3}), GX6 (2.69 g cm^{-3}), AX3 (2.66 g cm^{-3}) and WH3 (2.72 g cm^{-3}) of each collapsing gully, but the lowest in TC1 (2.58 g cm^{-3}), GX1 (2.57 g cm^{-3}), AX8 (2.53 g cm^{-3}) and WH1 (2.52 g cm^{-3}). Significant differences ($p<0.05$) were observed in the average PD values of the different soil layers in TC, GX, AX and WH (Figure 2 A). The PD was the least in the surface soil layer, followed by the detritus layer, which may be related to the higher humus content of the surface soil layer and the looser structure of detritus layer. In addition, the highest PD was observed in the red soil layer of TC, AX and WH and the sandy soil layer of GX, probably due to the large amounts of iron oxide and other heavy minerals they contain. Furthermore, as shown in Table 2, most of the soil PD values in all the four soil layers were less than 2.65 g cm^{-3}, which are often used to calculate the value of soil BD (Lee et al., 2009; Sharma and Bora PK, 2015). The lower PD value may be due to the loose structure of granite soil (Luk et al, 1997a).

3.1.2 Bulk density (BD)

From Table 2, it can also be seen that soil BD values were the lowest in the surface layer of all the collapsing gullies (1.29 g cm^{-3}, 1.27g cm^{-3}, 1.21 g cm^{-3} and 1.33 g $cm^{-3}$for TC, GX, AX and WH, respectively). However, relatively higher BD values were observed in the red soil layer (1.47 g cm^{-3}, 1.42 g cm^{-3}, 1.43 g cm^{-3} and 1.48 g cm^{-3} for TC, GX, AX and WH, respectively), followed by the sandy layer. The average soil BD values had significant difference ($p < 0.01$) in the different soil layers of TC, GX, AX and WH except in the surface layer of WH (Figure 2 B).Meanwhile, the bulk density first increased sharply ($p < 0.01$) and then declined slightly from the surface layer to the sandy soil layer of TC and to the detritus layer of GX, AX and WH (Table 2), which are similar to the report by Perrin et al. (2014). The soil BD values of the surface layer

Solid Earth Discuss., doi:10.5194/se-2016-152, 2016
Manuscript under review for journal Solid Earth
Published: 9 December 2016

were lower than those of the other layers, probably due to the higher content of SOM, more plant root distribution, better soil structure and texture (Choudhury et al., 2015). With the leaching and deposition process of the surface soil, the fine particles migrated to the red soil layer, leading to the filling of soil large pores and the increase of soil BD (Huang et al., 2014; Masto et al., 2015). The lower soil BD values of the sandy layer and detritus layer may be due to weak weathering and loose soil structure (Lan et al., 2013).

3.1.3 Total porosity (TP)

Unlike soil BD, the soil TP was comparatively high in the surface soil layer of GX and WH, but was the highest in the red soil layer of AX (Figure 2C). From Table 2, it can be seen that the soil TP values were lower in the red soil layer, such as the TC2 (44.11 %) and GX4 (46.02 %), which may be due to the weathering process of these soil layers, feldspar and mica in mineralized granites (Wang et al., 2015; Deng et al., 2016).

3.1.4 Soil organic matter (SOM)

Soil organic matter (SOM) plays an important role in soil nutrient availability, its increase may decrease the potential of soil erosion (Oliveira et al., 2015). As shown in Table 2, with the increase of depth, SOM contents in the soil layers of the four collapsing gullies showed a sharply decreasing trend (P<0.05). The sandy soil layers and detritus layers showed relatively lower SOM contents than those in the red soil layers and surface layers (Figure 2D). The AX1 had the highest SOM content (44.06 g kg^{-1}), followed by TC1 (23.37 g kg^{-1}), WH1 (15.17 g kg^{-1}) and AX2 (11.23 g kg^{-1}) (Table 2), which is mainly due to the decomposition of surface litter in the ground surface. However, the sandy soil layer and the detritus layer are basically in the state of incomplete weathering, and there is no accumulation of SOM (Xia et al., 2015).

3.1.5 Cation exchange capacity (CEC)

Cationic exchange capacity (CEC) is a measure of the soil capacity to adsorb and release cations (Jordán et al., 2009; Khaledian et al., 2016; Muñoz-Rojas et al., 2016). Similar to the SOM trend, CEC also decreased significantly from the upper soil layer to the bottom layer in the four collapsing gullies in TC, GX, AX and WH. As shown in Table 2, the CEC values were the highest in the surface soil layer of all the collapsing gullies (1.29 g cm^{-3}, 1.27g cm^{-3}, 1.21 g cm^{-3} and 1.33 g $cm^{-3}$for TC1, GX1, AX1 and WH1, respectively). The average CEC values in the four

Solid Earth Discuss., doi:10.5194/se-2016-152, 2016
Manuscript under review for journal Solid Earth
Published: 9 December 2016

collapsing gullies followed the order of surface soil layer> red soil layer> sandy soil layer> detritus layer with significant difference (P<0.05) (Figure 2E).

3.1.6 Free iron oxide (Fe_d)

Fe_d is the secondary product formed by the weathering of the parent rock during soil formation. One Fe_d state of the film surface is wrapped in the shape of clay minerals, and another state may be filled in the micropores of clay minerals (Cerdà et al., 2002; Lan et al., 2013). It is a unique and very important cementing material in weathered soil. As shown in Table 2, Fe_d values were the lowest in the detritus layer of all the collapsing gullies (11.89 g kg^{-1}, 9.41 g kg^{-1}, 7.30 g kg^{-1} and 8.37 g kg^{-1} for TC, GX, AX and WH, respectively). The highest Fe_d values of AX and WH were observed in the surface soil layer (31.03 g kg^{-1} and 28.40 g kg^{-1} for AX and WH), while those of TC and GX were observed in the red soil layer (27.37 g kg^{-1} and 26.59 g kg^{-1} for TC and GX). Overall, there are significant differences among surface soil layer, red soil layer, sandy soil layer and detritus layer in different weathering profiles (Figure 2F).These results show that the structural and mechanical properties are stronger in the surface soil layers and the red soil layers. However, when compared to the upper soil layers, the soil structure is loose and cohesive strength is low in the sandy soil layer and detritus layer.

3.1.7 Particle size distribution (PSD)

Soil particle size distribution (PSD) is one of the most important physical attributes in soil systems (Hillel, 1980). PSD affects the movement and retention of water, solutes, heat, and air, and thus greatly affects soil properties (Arjmand Sajjadi et al., 2014). The highest clay contents were 41.03, 36.65, 53.27 and 32.62% in TC, GX, AX and WH, respectively, and silt varied from 25.67 to 38.21% in TC, 28.43 to 38.68% in GX, 21.06 to 36.75% in AX and 26.90 to 41.51% in WH. The averages of particle size distributions for different weathering profiles of the four collapsing gullies are shown in Figure 3. The results indicated that the finer soil particles declined and the coarse soil particles increased from surface layer to detritus layer. The surface layer of TC, GX and WH collapsing gullies had the greatest clay content of 32.81, 36.65 and 32.62%, respectively, while the red soil layer of the AX collapsing gully showed the greatest clay content (45.63%). The reason for this phenomenon is the different weathering degree of granite, the grain size becomes coarser, the SiO_2 content and sand content increase, and the clay content decreases

Solid Earth Discuss., doi:10.5194/se-2016-152, 2016
Manuscript under review for journal Solid Earth
Published: 9 December 2016

from top to the bottom (Xu, 1996; Lin et al., 2015).

Insert: Table 2; Table 3 and Figure 2; Figure 3.

3.2 Soil Atterberg limits characteristics of weathering profiles of the collapsing gullies

All the measured soil plastic limit and liquid limit values varied significantly among the different soil layers in the four collapsing gullies (TC, GX, AX and WH). Table 4 lists the calculated values for the Atterberg limits, plasticity index and liquidity index. The average values for these properties are shown in Figure 4 and the relationship of these values with soil depth are shown in Figure 5.

3.2.1 Soil plastic limit and liquid limit

As shown in Table 4, soil plastic limit and liquid limit varied greatly from top to the bottom of different soil layers. Specifically, the soil plastic limit ranged from 19.43 % (TC6) to 35.93 % (TC1) with an average of 28.34 % in TC, 19.51 % (GX6) to 33.82 % (GX1) with an average of 24.19 % in GX, 19.32 % (AX7) to 36.03 % (AX2) with an average of 26.87 % in AX, and 18.91 % (WH8) to 36.56 % (WH8) with an average of 23.98 % in WH. Consistent with the variation trend of plastic limit, the soil liquid limit was found to be highest in TC1 (62.68 %), GX1 (57.70 %), AX1 (65.71 %) and WH1 (62.70 %) in each weathering profile of the four collapsing gullies, and lowest in TC6 (30.91 %), GX6 (30.89 %), AX8 (32.48 %) and WH7 (30.77 %). The averages of soil plastic limit and liquid limit are shown in Table 4. The results indicated that, with declining weathering degree (from surface layer to detritus layer), the plastic limit and liquid limit decreased noticeably ($p<0.05$) (Figure 5A; 7B). The surface layer of all the four collapsing gullies had the greatest soil Atterberg limits (35.93, 33.82, 35.58 and 36.56 % for the plastic limit, and 62.68, 57.70, 65.71 and 62.70 % for the liquid limit, respectively). The plastic limit of the sandy soil layer and the detritus layer was significantly lower ($p<0.01$) than that of the surface soil layer and the red soil layer, but with no significant difference between each other. As shown in Figure 5, the soil Atterberg limits presented a nonlinear relationship with soil depth. Power function fitting showed that both the soil plastic limit and liquid limit had a remarkable negative correlation with the soil depth (Figure 5A, $R^2=0.784$, $p<0.001$ and Figure 5B, $R^2=0.877$, $p<0.0001$, respectively). Additionally, the soil plastic limit of the surface soil layer and the red soil layer ranged between 24.70 % and 36.56 % with an average of 31.98 % and the liquid limit ranged between 49.43 % and 65.71 % with an average of 57.02 %,

Solid Earth Discuss., doi:10.5194/se-2016-152, 2016
Manuscript under review for journal Solid Earth
Published: 9 December 2016

which are higher compared with most types of soil (Reznik, 2016), but an opposite trend was observed in the sandy soil layer and the detritus layer. The soil plastic limit and liquid limit are respectively the minimum water content and the maximum water content of the soil in the plastic state, which reflect the strength of the connection between soil particles and the resistance ability of the soil to the deformation caused by the external force when the water content is different (Institute of Soil Science, Chinese Academy of Sciences, 1978). Our findings are in agreement with the previous studies by Zhuang et al. (2014) and Xia et al. (2016), which reported the upper soil layer has a better ability to resist deformation than the bottom layer. These results indicate that the change of water content has little influence on the surface soil layer and the red soil layer, and the soil cannot be easily transformed into a liquid state by the rainfall erosion and runoff scouring. Conversely, the change of water content has a great influence on the sandy soil layer and the detritus layer, and with water content increasing, the soil can be changed from solid to liquid state.

3.2.2 Soil plasticity index and liquidity index

Soil plasticity index is an indicator for the difference between liquid limit and plastic limit, while liquidity index represents the ratio of the difference of the natural moisture content and the plastic limit to the plastic limit (Zhuang et al., 2014). These indexes were calculated by formulae (1) and (2). As shown in Table 4, there are considerable differences in soil plasticity index and liquidity index among the different weathering profiles of the four collapsing gullies. The soil plasticity index was highest in AX1 (30.14 %), followed by TC1 (26.75 %), GX3 (26.50 %) and WH2 (26.19 %), and it also was the highest in each soil layer. However, the plasticity index was lowest in the bottom soil layers (11.48, 10.09 and 11.53% for TC6, GX8 and AX8, respectively) except for WH. Additionally, inconsistent with plasticity index, liquidity index was the lowest in the surface soil layer of each weathering profile (-49.55, -50.36, -64.57 and -65.91 % for TC1, GX1, AX1 and WH1, respectively). The highest liquidity indexes of TC, GX, AX and WH were -10.57 % in TC6, -17.61 % in GX8, -12.41 % in AX8 and -11.65 % in WH7, respectively. Figure 4 summarizes the statistics of soil plasticity index and liquidity index in all of the different weathering profiles of the four collapsing gullies. Significant differences were observed among the surface soil layer, red soil layer, sandy soil layer and the detritus layer for all the measured plasticity and liquidity indexes. The results indicated that the soil plasticity index decreased noticeably with the decline of weathering degree

Solid Earth Discuss., doi:10.5194/se-2016-152, 2016
Manuscript under review for journal Solid Earth
Published: 9 December 2016

348 (from surface layer to detritus layer), which is similar to the variation regularity of plastic limit and
349 liquid limit.

350 The surface layer of the TC, AX and WH collapsing gullies had the greatest soil plasticity index
351 (26.75%, 30.14 % and 26.14 %, respectively), but the greatest plasticity index (23.88%) of the GX
352 collapsing gully was found in the red soil layer. In contrast with the plasticity index, the liquidity
353 index was significantly ($p<0.05$) higher in the sandy soil layer and the detritus layer and was the
354 lowest in the surface soil layer (-49.55 %, -50.36 %, -64.57 % and -65.91 % for TC, GX, AX and
355 WH, respectively) (Figure 4). Regression analyses were performed to determine the strength of
356 relationships between the plasticity index, the liquidity index and soil depth (Figure 5). The
357 nonlinear regression analyses showed that the plasticity index had a remarkable negative correlation
358 with the soil depth (Figure 5C, $R^2=0.759$, $p<0.0001$). However, there was a significant positive
359 correlation between the soil liquidity index and the soil depth based on the power function fitting
360 analysis (Figure 5D, $R^2=0.382$, $p<0.05$).

361 The differences in soil plasticity index and liquidity index between upper layer and lower layer
362 may be related to the variation in the dynamics of the soil properties. As previously reported [64],
363 changes in soil plasticity index and liquidity index depend on soil properties. The plasticity index
364 reflects the range of the soil water content when the soil is in the plastic state. The size of the
365 plasticity index is directly related to the maximum possible bound water content of a certain mass
366 of soil particles. The greater the maximum possible bound water content is, the greater the
367 plasticity index will be. However, the bound water content of soil is related to the size of soil
368 particle, mineral composition, the composition and concentration of cation in the hydration
369 membrane. Thus, the plasticity index is a comprehensive indicator for the reaction properties of
370 clayey soil, which means the larger the index is, the higher the clay content will be (Husein et al.,
371 1999). Our findings clearly demonstrated that the plasticity index of lower soil layers was
372 significantly lower ($p<0.01$) than that of the upper layers in the different weathering profiles of the
373 four collapsing gullies, implying that the content of fine particles in the soil gradually decreased
374 with soil depth. Previous studies about soil texture classification are frequently based on soil
375 plasticity index: the soil with a value between 10% and 17% is defined as silty clay and that with a
376 value greater than 17% is classified as clay (Zentar et al., 2009; Marek et al., 2015). Therefore,

Solid Earth Discuss., doi:10.5194/se-2016-152, 2016
Manuscript under review for journal Solid Earth
Published: 9 December 2016

based on this classification theory, most soil layers in the TC, GX, AX and WH collapsing gullies can be defined as clay, while the lower soil layers can be classified as silty clay, which is more susceptible to erosion.

However, the adsorption capacity of bound water varied under a different soil specific surface area and mineral composition. Therefore, given the same water content, for the soil with high viscosity, the water may be bound water, while for the soil with low viscosity, a considerable part of the water can be free water, which means that the soil state cannot be defined only by water content and we need another indicator, namely the liquidity index, to reflect the relationship between natural water content and Atterberg limits in the soil. The liquidity index is defined as the ratio of the difference between the natural moisture content and the plastic limit to the plastic limit (Sposito, 1989). When the natural moisture content is close to the plastic limit, the soil is hard; and when it is close to the liquid limit, the soil is weak. In engineering practice, the soil is in a hard state when the liquidity index is less than 0 (Zhuang et al., 2014). In our research, the liquidity indexes of all soils were less than 0, indicating that the soil of the different weathering profiles of the four collapsing gullies is hard in the natural state. Nevertheless, the lower soil layer of the collapsing gullies is more close to 0 than the upper layer in the liquidity index, indicating that the lower soil is weaker than the upper layer soil.

Insert: Table 4 and Figure 4; Figure 5.

3.2.3 Relationship between soil Atterberg limits and collapsing gully

The ability of soil to resist external erosion varies with soil Atterberg limits. In this study, the liquidity indexes of all soils were less than 0, indicating that the soils of the four collapsing gullies remain solid in natural state, with a high shear strength and strong resistance to water erosion, enabling the soil of granite weathering profile to maintain stability. From the soil Atterberg limits of all the soils of the four collapsing gullies, it can be seen that the plastic limit, liquid limit and plasticity index are higher in the surface soil layer and red soil layer, implying that the plastic state cannot be easily changed when the rain lasts a short time such as moderate to light rain, which usually does not lead to the collapse and loss of the soils with high compaction and hardness. However, if the rainfall duration continues long enough, the soil water content can reach a high level, leading to the increase of the soil self-weight, the decrease of the soil shear strength, and then

Solid Earth Discuss., doi:10.5194/se-2016-152, 2016
Manuscript under review for journal Solid Earth
Published: 9 December 2016

the collapse of the soils. The plastic limit, liquid limit and plasticity index of the sandy soil layer and detritus layer of the collapsing gully are significantly smaller than those of the surface soil layer and red soil layer, indicating that it is very easy for the soils to reach the plastic limit in the case of short-term rainfall, and coupled with the looser soil and smaller soil shear strength, it is easy for them to collapse.

Because of the lower soil Atterberg limits of the collapsing gully in the bottom soil layers, soil moisture absorption leads to the increase of water content after a long time of rain erosion and soil preferential flow. The sandy soil layer and detritus layer of the collapsing gully would be the first to reach or close to the plastic state in the same moisture conditions. Meanwhile, the shear strength of the two soil layers decreased rapidly, leading to the formation of the weak surface and then the collapse or water erosion. The erosion is much more serious in the sandy soil layer and detritus layer than in the surface soil layer and red soil layer, resulting in the hollow-out of the lower soil layers and the formation of a concave pit called "niche" in the engineering geology (Ding et al., 1995; Deng et al., 2016). The formation and development of the niche is the preliminary stage of the formation of a collapsing gully. After niche formation, the surface soil layer and red soil layer lack support, giving rise to a total collapse by the soil self-weight. The occurrence of collapse forms the source of erosion, resulting in the formation of the collapsing gully.

3.3 Effect of soil physico-chemical properties on soil Atterberg limits

In this research, we examined the soil particle density (PD), bulk density (BD), total porosity (TP), soil organic matter (SOM) , cation exchange capacity (CEC), free iron oxide (Fe_d) and particle size distribution (PSD) among the different soil layers in the four collapsing gullies (TC, GX, AX and WH). The relationship between soil physico-chemical properties and soil Atterberg limits are shown in Table 4 and Figure 6.

Insert: Table 5 and Figure 6.

3.3.1 Soil particle density (PD), bulk density (BD) and total porosity (TP)

Regression analyses were performed to determine the strength of relationships between Atterberg limits and soil particle density, bulk density and total porosity in the soil of the four collapsing gullies (TC, GX, AX and WH). In the four collapsing gullies, soil Atterberg limits had a very weak negative correlation with the soil BD (R^2= 0.044, $p<0.05$ for plastic limit; R^2= 0.021, $p<0.05$ for

Solid Earth Discuss., doi:10.5194/se-2016-152, 2016
Manuscript under review for journal Solid Earth
Published: 9 December 2016

liquid limit) and PD (R^2= 0.023, p<0.05 for plastic limit; R^2= 0.002, p<0.05 for liquid limit), and a very weak positive correlation with the soil TP (R^2= 0.117, p<0.05 for plastic limit; R^2= 0.074, p<0.05 for liquid limit). Therefore, there was almost no significant correlation between soil Atterberg limits and PD, BD and TP in the soils of the four collapsing gullies.

3.3.2 Soil organic matter (SOM)

In reference to Figure 6, regression analyses showed that the soil organic matter had a significant positive correlation with plastic limit (R^2=0.816, P<0.01) and liquid limit (R^2=0.785, P<0.01) in all of the different weathering profiles of the four collapsing gullies. This may be due to the reason that soil organic matter can promote organic colloid formation, which can affect the specific surface area, the water holding capacity of the soil particles and then the soil liquid limit (Stanchi et al., 2012). With the increase of organic matter content, organic colloid also increased, indicating/implying that the greater the water holding capacity of the soil is, the greater the liquid limit will be. In our research, the soil Atterberg limits had a significant positive correlation with the organic matter in all of the different weathering profiles. Similar results were also reported by Zhuang et al. (2014) and Husein et al (1999), who both concluded that the plastic limit and the liquid limit of the soil increase with increasing organic content. According to the relationship between the Atterberg limits and the organic matter in the weathering profiles of the granite soil, we can conclude that the higher the content of organic matter is, the stronger the anti-erodibility of the soil will be. Thus, our research provides a theoretical basis for the prevention and control of collapsing gully erosion by planting green manure to improve soil organic matter in these areas.

3.3.3 Cation exchange capacity (CEC)

As shown in Figure 6, there was a strong positive correlation between soil Atterberg limits and CEC (R^2= 0.636, p<0.01 for plastic limit; R^2= 0.739, p<0.01 for liquid limit). Similar results were reported by Cathy et al. (2008), who put forward that CEC can be an indicator for the mineral type and is highly correlated to plastic limit and liquid limit.

3.3.4 Free iron oxide (Fe_d)

A positive significant correlation was observed between soil Atterberg limits and Fed (R^2= 0.630, p<0.01 for plastic limit; R^2= 0.788, p<0.01 for liquid limit) (Figure 6). This is consistent with the finding of Stanchi (2015), who reported that Atterberg limits were also affected by CEC. Therefore,

Solid Earth Discuss., doi:10.5194/se-2016-152, 2016
Manuscript under review for journal Solid Earth
Published: 9 December 2016

464 Fe_d acts as an inorganic binding agent in structure formation, and participates in reducing horizon
465 vulnerability, as proposed by Sposito (1989).

466 **3.3.5 Particle size distribution (PSD)**

467 Regression analyses were performed to determine the strength of relationships between soil
468 Atterberg limits and the contents of gravel, coarse sand, fine sand, silt and clay in the soils of
469 collapsing gullies (Figure 6). The non-linear regression analyses showed a strong positive
470 correlation of the soil Atterberg limits with the clay content (R^2= 0.736, $p<0.01$ for plastic limit;
471 R^2= 0.820, $p<0.01$ for liquid limit), a remarkable negative correlation with the content of sand
472 (R^2= 0.580, $p<0.01$ for plastic limit; R^2= 0.616, $p<0.01$ for liquid limit) and a weak negative
473 correlation with the silt content (R^2= 0.320, $p<0.05$ for plastic limit; R^2= 0.210, $p<0.05$ for liquid
474 limit), gravel content (R^2= 0.255, $p<0.05$ for plastic limit; R^2= 0.202, $p<0.05$ for liquid limit),
475 coarse sand content (R^2= 0.214, $p<0.05$ for plastic limit; R^2= 0.374, $p<0.05$ for liquid limit) and
476 fine sand content (R^2= 0.131, $p<0.05$ for plastic limit; R^2= 0.158, $p<0.05$ for liquid limit). The
477 significant negative correlation between soil Atterberg limits and sand may be attributed to
478 porosity and specific surface area. When the sand content increases, the soil pores will increase
479 and surface area will decrease, resulting in poor soil performance and facilitating water
480 movement. Meanwhile, sandy soil is low in viscosity, loose and difficult to expand, leading to the
481 slow rise of capillary water during water erosion. Therefore, the soil plastic limit and liquid limit
482 will decrease with increasing sand content. Our results show that with declining weathering degree
483 (from surface layer to detritus layer), the sand increased and the finer soil particles declined,
484 which causes the decrease of soil Atterberg limits, and the lower soil layers are the first to be
485 eroded (Zhuang et al., 2014).

486 Furthermore, there was a significant positive correlation between soil Atterberg limits and clay
487 content, indicating that the clay content, despite its modest amount, plays a major role in
488 determining the values of plastic limit and liquid limit. This also shows that, in the weathering
489 profiles, the soil Atterberg limits increased with the increase of clay content, which is also reported
490 by several other studies (Polidori, 2007; Baskan et al., 2009; Keller and Dexter, 2012). This result
491 may be due to the effect of clay on soil plasticity in changing the arrangement of soil particles. The
492 connection form, the arrangement of soil particles and soil pore size will vary greatly with the clay

Solid Earth Discuss., doi:10.5194/se-2016-152, 2016
Manuscript under review for journal Solid Earth
Published: 9 December 2016

493 content. Additionally, soil clay has a larger specific surface area, which will affect the soil water
494 storage capacity. Therefore, the huge specific surface area enables the clay to have strong
495 adsorption capacity, which affects the speed of water flow in the soil. Meanwhile, the mosaic of
496 clay particles to the larger pores can also block the flow channels in the soil. All of these will
497 affect the soil Atterberg limits, with the high clay content contributing to the directional
498 arrangement of soil particles, leading to the increase of weak bound water content, thereby
499 increasing the plastic limit and liquid limit of the soil.

500 Overall, soil is a spheres of the earth system with special structure and function. From the point
501 of view of the earth's circle, soil science should not only study the soil material, but also should
502 change towards the relationship between the soil and the earth's circle, which has a profound
503 impact on human living environment and global change research (Brevik et al., 2015; Keesstra et
504 al., 2016). The results show that the relationship between soil Atterberg limits and the occurrence
505 mechanism of collapsing gully, which can be used as a reference for the assessment of natural
506 disasters occurring in the interaction between water and force in nature.

507 **4 Conclusions**

508 Based on the analyses of soil Atterberg limits, soil physico-chemical properties, the influence
509 factors on collapsing gully and the relationships between soil Atterberg limits and soil physico-
510 chemical properties of different weathering profiles of the four collapsing gullies in the hilly granitic
511 region, the conclusions are summarized as follows:

512 Different weathering profiles exhibit a significant effect on soil Atterberg limits and soil physico-
513 chemical properties. The upper soil layers (surface layer or red soil layer) of all the collapsing gullies
514 show the highest plastic limit, liquid limit, plasticity index, SOM, CEC, Fe_d, finer soil particles and
515 the lowest liquidity index, PD, and BD. With the fall of weathering degree (from surface layer to
516 detritus layer), there is a sharp decrease in the plastic limit, liquid limit, plasticity index, SOM, CEC
517 and Fe_d, a gradual increase in liquidity index, a sharp increase in PD and BD first followed by a
518 slight decline. Additionally, the finer soil particles (silt and clay) decrease, and especially the clay
519 contents decline noticeably, whereas the gravel and sand contents increase considerably. Therefore,
520 the soils of bottom layers are very easy to reach the soil Atterberg limits during rain, and coupled
521 with the looser soil structure, they are easy to be eroded, resulting in the hollow-out of these soil

522 layers and the formation of a concave pit called "niche" in engineering geology. After the niche
523 formation, the upper soil layers lack support, leading to a total collapse in the soil by the soil self-
524 weight. The collapse occurrence forms the source of erosion, causing the formation of the collapsing
525 gully. The regression analysis shows that soil Atterberg limits are significantly positively correlated
526 with SOM, clay content, CEC and Fe_d, remarkably negatively correlated with sand content and not
527 obviously correlated with other properties. The results of this study demonstrate that soil Atterberg
528 limits can be regarded as an informative indicator to reflect the weathering degree of different
529 weathering profiles of the collapsing gully. Future research will include the relationship between
530 soil Atterberg limits and soil mechanical properties.
531
532 *Author contributions.* Conceived and designed the experiments: Y. S. Deng, C. F. Cai and J. Z.
533 Chen. Performed the experiments: Y. S. Deng and D. Xia. Analyzed the data: Y. S. Deng.
534 Contributed reagents/materials/analysis tools: Y. S. Deng, D. Xia and S. W. Ding. Wrote the
535 paper: Y. S. Deng, C. F. Cai, D. Xia, S. W. Ding and J. Z. Chen.
536
537 *Acknowledgements.* Financial support for this research was provided by the National Natural
538 Science Foundation of China (No.41630858; 41601287 and 41571258) and National Science and
539 technology basic work project (No.2014 FY110200A16). We would like to thank several
540 anonymous reviewers for their valuable comments on the previous version of the manuscript.
541 Finally, thanks to all of our colleagues who supported the undertaking of this work.
542
543 **References**
544 Anderson, J. M., and Ingram, J. S. I.: Tropical soil biology and fertility: a handbook of methods, Soil Sci., 157,
545 265, 1994.
546 Archer J.R.: Soil consistency. In: Soil Physical Conditions and Crop Production. Ministry of Agriculture, Fisheries
547 and Food, Tech. Bull. 29. London: HMSO. pp 289-297, 1975.
548 Arjmand Sajjadi, S., and Mahmoodabadi, M.: Aggregate breakdown and surface seal development influenced by
549 rain intensity, slope gradient and soil particle size. Solid Earth, 6, 3303-3331, 2014.
550 Armo, L. V., Agata, N., Vito, B., Markus, E., and Luigi, B.: Long-term tillage and cropping system effects on

chemical and biochemical characteristics of soil organic matter in a Mediterranean semiarid environment, Land Degrad. Dev., 26, 45-53, 2015.

ASTMD 4318-10e1.: Standard Test Methods for Liquid Limit, Plastic Limit, and Plasticity Index of Soils. ASTM International, West Conshohocken, PA, 2010.

Atterberg A.: Die plastizität der tone, Internationale Mitteilungen für Bodenkunde, 1, 10-43, 1911.

Baskan, O., Erpul, G., and Dengiz, O.: Comparing the efficiency of ordinary Kriging and cokriging to estimate the Atterberg limits spatially using some soil physical properties, Clay Miner., 44, 181-193, 2009.

Baver L.D.: The Atterberg consistency constants: Factors affecting their values and a new concept of their significance, Journal of the American Society of Agronomy, 22, 935-948, 1930.

Brevik, E. C., Cerdà, A., Mataix-Solera, J., Pereg, L., Quinton, J. N., Six, J., and Van Oost, K.: The interdisciplinary nature of SOIL, SOIL, 1, 117-129, doi:10.5194/soil-1-117-2015, 2015.

Campbell D.J.: Liquid and plastic limits. In: Soil and environmental analysis-physical methods (eds K.A. Smith & C.E. Mullins). Dekker Inc., New York. pp. 349-375, 2001.

Casagrande A.: Notes on the design of the liquid limit device, Geótechnique, 8, 84-91, 1958.

Casagrande A.: Research on the Atterberg limits of soils, 13, 121-136, 1932.

Cathy, A., Elrashidi, Moustafa, A., Engel, and Robert, J.: Linear regression models to estimate soil liquid limit and plasticity index from basic soil properties. Soil Sci., 173, 25-34, 2008.

Cerdà, A. and Doerr, S. H.: Soil wettability, runoff and erodibility of major dry-Mediterranean land use types on calcareous soils, Hydrol. Process., 21, 2325-2336, 2007.

Cerdà, A., and Doerr, S. H.: The effect of ant mounds on overland flow and soil erodibility following a wildfire in eastern spain, Ecohydrology, 3, 392-401, 2010.

Cerdà, A.: The effect of season and parent material on water erosion on highly eroded soils in eastern Spain, J. Arid Environ., 52, 319-337, 2002.

Choudhury, B. U., Fiyaz, A. R., Mohapatra, K. P., and Ngachan, S.: Impact of land uses, agrophysical variables and altitudinal gradient on soil organic carbon concentration of North-eastern Himalayan region of India, Land Degrad. Dev., doi: 10.1002/ldr.2338, 2016.

Curtaz, F., Stanchi, S., D'Amico, M. E., Filippa, G., Zanini, E., and Freppaz, M.: Soil evolution after land-reshaping in mountains areas (Aosta Valley, NW Italy), Agr. Ecosyst. Environ., 199, 238-248, 2015.

Deng Y.S., Ding S.W., Cai C.F., Lv G.A.: Characteristic curves and model analysis of soil moisture in collapse

Solid Earth Discuss., doi:10.5194/se-2016-152, 2016
Manuscript under review for journal Solid Earth
Published: 9 December 2016

mound profi les in southeast Hubei. Acta Pedologica Sinica 53:355-364, 2016 (in Chinese).

Deng Y.S., Ding S.W., Liu C.M., Xia D., Zhang X.M., Lv G.A.: Soil moisture characteristics of collapsing gully wall in granite area of southeastern Hubei, J. soil Water Conserv., 29, 132-137, 2015 (in Chinese).

Deng Y.S., Xia D., Cai C.F., Ding S.W.: Effects of land uses on soil physic-chemical properties and erodibility in collapsing-gully alluvial fan of Anxi County, China, J. Integr. Agr., 15, 1863-1873, 2016.

Ding S.W., Cai C.F., Zhang G.Y.: A study on gravitational erosion and the formation of collapsing gully in the granite area of Southeast Hubei, Journal of Nanchang College of Water Conservancy and Hydroelectric Power, S1, 50-54, 1995 (in Chinese).

Douglas, G. B., Mcivor, I. R., Manderson, A. K., Koolaard, J. P., Todd, M., and Braaksma, S., et al.: Reducing shallow landslide occurrence in pastoral hill country using wide-spaced trees, Land Degrad. Dev., 24, 103–114, 2013.

Feng M. H., Liao C. Y., Li S. X. and Lu S. L.: Investigation on the present situation of collapsing gully in the south of China, People Yangtze River, 40, 66-68,2009 (in Chinese).

Gao Y., Zhong B., Yue H., Wu B. and Cao S.: A degradation threshold for irreversible soil productivity loss in southeastern China: results of a long-term case study in Changting County, J. Applied Ecolo., 48, 1145-1154, 2011.

Gee G. W. and Bauder J. W.: Particle size analysis. In: Klute, A. (Ed.), Methods of Soil Analysis, Part 1. Agronomy, 9. Am. Soc. Agron. Inc., Madison, Wis, 1986.

Hillel D.: Fundamentals of Soil Physics. Academic Press: New York, 1980.

Huang B., Li Z., Huang J., Liang G., Nie X. and Wang Y, et al.: Adsorption characteristics of Cu and Zn onto various size fractions of aggregates from red paddy soil, Journal of Hazardous Materials, 264, 176-183, 2014.

Husein Malkawi, A. I., Alawneh, A. S., and Abu, O. T.: Effects of organic matter on the physical and the physicochemical properties of an illitic soil, Appl. Clay Sci., 14, 257-278, 1999.

Institute of Soil Science, Chinese Academy of Sciences.: Physical and Chemical Analysis of Soils. Shanghai Science and Technology Press, Shanghai, 1978 (in Chinese).

Jiang F. S., Huang Y. H., Wang M. K., Lin J. S., Zhao F. and Ge H.L.: Effects of rainfall intensity and slope gradient on steep colluvial deposit erosion in southeast China, Soil Sci. Soc. Am. J., 78, 1741-1752, 2014.

Jong, E. D., Acton, D. F., and Stonehouse, H. B.: Estimating the Atterberg limits of southern Saskatchewan soils from texture and carbon contents. Can. J. Soil Sci., 70, 543-554, 1990.

609 Jordán, A., Ángel J. Gordillo-Rivero, García-Moreno, J., Zavala, L. M., Granged, A. J. P., and Gil, J., et al.: Post-
610 fire evolution of water repellency and aggregate stability in Mediterranean calcareous soils: a 6-year study,
611 Catena, 118, 115-123, 2014.
612 Jordán, A., Zavala, L. M., Nava, A. L., and Alanís, N.: Occurrence and hydrological effects of water repellency in
613 different soil and land use types in Mexican volcanic highlands, Catena, 79, 60-71, 2009.
614 Keesstra, S. D., Bouma, J., Wallinga, J., Tittonell, P., Smith, P., Cerdà, A., Montanarella, L., Quinton, J. N.,
615 Pachepsky, Y., van der Putten, W. H., Bardgett, R. D., Moolenaar, S., Mol, G., Jansen, B., and Fresco, L. O.:
616 The significance of soils and soil science towards realization of the United Nations Sustainable Development
617 Goals, SOIL, 2, 111-128, doi:10.5194/soil-2-111-2016, 2016.
618 Keller, T., and Dexter, A. R.: Plastic limits of agricultural soils as functions of soil texture and organic matter
619 content, Soil Res., 50, 7-17, 2012.
620 Khaledian, Y., Kiani, F., Ebrahimi, S., Brevik, E. C., and Aitkenhead-Peterson, J.: Assessment and monitoring of
621 soil degradation during land use change using multivariate analysis, Land Degrad. Dev., doi: 10.1002/ldr.2541,
622 2016.
623 Lan, H. X., Hu, R. L., Yue, Z. Q., Lee, C. F., and Wang, S. J.: Engineering and geological characteristics of granite
624 weathering profiles in South China, J. Asian Earth Sci., 21, 353-364, 2003.
625 Lee, S. B., Chang, H. L., Jung, K. Y., Park, K. D., Lee, D., and Kim, P. J.: Changes of soil organic carbon and its
626 fractions in relation to soil physical properties in a long-term fertilized paddy, Soil Till. Res., 104, 227-232,
627 2009.
628 Li S. P.: Study on erosion law and control of slope disintegration in Guangdong province, Journal of natural
629 disasters, 3, 68-74, 1992 (in Chinese).
630 Liang Y., Ning D. H., Pan X. Z., Li D. C. and Zhang B.: Characteristics and treatment of collapsing gully in red
631 soil region of southern China, Soil and water conservation in China, 1, 31-34, 2009.
632 Lin J. S., Huang Y. H., Wang M. K., Jiang, F. S., Zhang X. and Ge H.: Assessing the sources of sediment
633 transported in gully systems using a fingerprinting approach: An example from South-east China, Catena, 129,
634 9-17, 2015.
635 Liu X. L. and Zhang D. L.: Distribution Characteristics and spatial variation of Benggang soil moistures: A case
636 study of Liantanggang in Wuhua County, Guangdong, Tropical Geography, 35, 291-297, 2015 (in Chinese).
637 Luk, S. H., Dicenzo, P. D., and Liu, X. Z.: Water and sediment yield from a small catchment in the hilly granitic

region, South China, Catena, 29, 177-189, 1997b.

Luk, S. H., Yao, Q. Y., Gao, J. Q., Zhang, J. Q., He, Y. G., and Huang, S. M.: Environmental analysis of soil erosion in Guangdong province: a Deqing case study, Catena, 29, 97-113, 1997a.

Marek S. Żbik, David J. Williams, Yen-Fang Song, and Chun-Chieh Wang.: Smectite clay microstructural behaviour on the Atterberg limits transition. Colloid Surface A., 467, 89-96, 2015.

Masto, R. E., Sheik, S., Nehru, G., Selvi, V. A., George, J., and Ram, L. C.: Assessment of environmental soil quality around Sonepur Bazari mine of Raniganj coalfield, India, Solid Earth, 6, 811-821, 2015.

McBride R.A.: Soil consistency and lower plastic limits. In:Carter MR, Gregorich EG (eds.), Soil Sampling and Methods of Analysis, 2nd edition, Chapter n58, CRC Press. pp 761-769, 2008.

Mehra, O.P. and Jackson, M.L.: Iron oxide removal from soils and clays by a dithionite-citrate system buffered with sodium bicarbonate, Clays Clay Miner, 7, 317-327, 1958.

MorenoRamón, H., Quizembe, S. J., and IbáñezAsensio, S.: Coffee husk mulch on soil erosion and runoff: experiences under rainfall simulation experiment, Solid Earth, 5, 851-862, 2014.

Muñoz-Rojas, M., Erickson, T. E., Dixon, K. W. and Merritt, D. J.: Soil quality indicators to assess functionality of restored soils in degraded semiarid ecosystems, Restoration Ecology, 24, S43-S52, 2016.

Muñoz-Rojas, M., Erickson, T. E., Martini, D., Dixon, K. W. and Merritt, D. J.: Soil physicochemical and microbiological indicators of short, medium and long term post-fire recovery in semi-arid ecosystems, Ecological Indicators, 63, 14-22, 2016.

Nelson D. W. and Sommers L.E.: Total carbon, organic carbon, and organic matter. Methods of Soil Analysis Part-chemical Methods, 1982.

Oliveira, S. P. D., Lacerda, N. B. D., Blum, S. C., Escobar, M. E. O., and Oliveira, T. S. D.: Organic carbon and nitrogen stocks in soils of northeastern Brazil converted to irrigated agriculture, Land Degrad. Dev., 26, 9-21, 2015.

Pavlova, I., Jomelli, V., Brunstein, D., Grancher, D., Martin, E., and Déqué, M.: Debris flow activity related to recent climate conditions in the French Alps: a regional investigation, Geomorphology, 219, 248-259, 2014.

Peng, F., Quangang, Y., Xue, X., Guo, J., and Wang, T.: Effects of rodent-induced land degradation on Ecosytem carbon fluxes in alpine meadow in the Qinghai-Tibet plateau, China, Solid Earth, 6, 303-310, 2015.

Perrin, A. S., Fujisaki, K., Petitjean, C., Sarrazin, M., Godet, M., and Garric, B., et al.: Conversion of forest to agriculture in Amazonia with the chop-and-mulch method: does it improve the soil carbon stock? Agr. Ecosyst.

667 Environ., 184, 101-114, 2014.
668 Polidori E.: Relationship between the Atterberg limits and clay content, Soils Found., 47, 887-896, 2007.
669 Qiu S.J.: The process and mechanism of red earth slope disintegration erosion, Bulletin of soil and Water
670 Conservation, 6, 31-40, 1994 (in Chinese).
671 Rashid, A. S. A., Kalatehjari, R., Noor, N. M., Yaacob, H., Moayedi, H., and Sing, L. K.: Relationship between
672 liquidity index and stabilized strength of local subgrade materials in a tropical area, Measurement, 55, 231-237,
673 2014.
674 Reznik, Y. M.: Relationship between plastic limit values and fine fractions of soils. Geotechnical and Geological
675 Engineering, 34, 403-410, 2016.
676 Rhoades J. D.: Cation exchange capacity. In: Page, A.L. _Ed.., Methods of Soil Analysis, Part 2, Chemical and
677 Microbiological Properties, 2nd edn. Agronomy 9. ASA, SSSA. Madison, WI, USA, pp.149-157, 1982.
678 S.I.S.S.: In: Angeli Milano, Franco (Ed.), Metodi di analisi fisica del suolo, 1997.
679 Shahminan, D. N. I. A. A., Rashid, A. S. A., Bunawan, A. R., Yaacob, H., and Noor, N. M.: Relationship between
680 strength and liquidity index of cement stabilized laterite for subgrade application, International Journal of Soil
681 Science, 9, 16-21, 2014.
682 Sharma B. and Bora P. K.: A study on correlation between liquid limit, plastic limit and consolidation properties of
683 soils, Indian Geotechnical Journal, 45, 1-6, 2015.
684 Sheng J. A. and Liao A. Z.: Erosion control in south China, Catena, 29, 211-221, 1997.
685 Sposito G.: The Chemistry of Soils. Oxford Univ. Press, New York, 1989.
686 Stanchi, S., D'Amico, M., Zanini, E., and Freppaz, M.: Liquid and plastic limits of mountain soils as a function of
687 the soil and horizon type, Catena, 135, 114-121, 2015.
688 Stanchi, S., Freppaz, M., and Zanini, E.: The influence of alpine soil properties on shallow movement hazards,
689 investigated through factor analysis. Nat. Hazard Earth Sys., 12, 1845-1854, 2012.
690 Vacchiano G., Stanchi S., Ascoli D., Marinari G., Zanini E. and Motta R.: Soil-mediated effects of fire on Scots
691 pine (Pinussylvestris L.) regeneration in a dry, inner-alpinevalley. Sci. Total Environ., 472, 778-788, 2014.
692 Wang Y. H., Xie X. D. and Wang C. Y.: Formation mechanism of calamities due to Benggang processes of
693 weathered granitic rocks, Journal of mountain science, 6, 496-501, 2000.
694 Wang, C., Yang, Y., and Zhang, Y.: Cost-effective targeting soil and water conservation: a case study of Changting
695 County in Southeast China. Land Degrad. Dev, 2016, DOI: 10.1002/ldr.2397.

Solid Earth Discuss., doi:10.5194/se-2016-152, 2016
Manuscript under review for journal Solid Earth
Published: 9 December 2016

696 Wroth C. P. and Wood, D. M.: The correlation of index properties with some basic engineering properties of soils,
697 Canadian Geotechnical Journal, 15, 137-145, 1978.
698 Xia, D., Deng, Y. S., Wang, S. L., Ding, S.W., and Cai, C. F.: Fractal features of soil particle-size distribution of
699 different weathering profiles of the collapsing gullies in the hilly granitic region, South China, Nat. Hazards, 79,
700 455-478, 2015.
701 Xu J. X.: Benggang erosion: the influencing factors, Catena, 27, 249-263, 1996.
702 Yalcin A.: The effects of clay on landslides: a case study, Appl. Clay Sci., 38, 77-85, 2007.
703 Zeng Z. X.: Rock topography. Geological Publishing House, 1980 (in Chinese).
704 Zentar R., Abriak N. E. and Dubois V.: Effects of salts and organic matter on Atterberg limits of dredged marine
705 sediments, Appl. Clay Sci., 42, 391-397, 2009.
706 Zhang S. and Tang H. M. Experimental study of disintegration mechanism for unsaturated granite residual soil,
707 Rock and Soil Mechanics, 6, 1668-1674, 2013 (in Chinese).
708 Zhang X. J.: The practice and prospect of hill collapsing improving and development in southern China, China
709 Water Resource, 4, 17-22, 2010. (in Chinese).
710 Zhang X. M., Ding S. W. and Cai C.F.: Effects of drying and wetting on nonlinear decay of soil shear strength in
711 slope disintegration erosion area. Transactions of the Chinese Society of Agricultural Engineering, 28, 241-245,
712 2012 (in Chinese).
713 Zhong B. L., Peng S. Y., Zhang Q., Ma H. and Gao S. X.: Using an ecological economics approach to support the
714 restoration of collapsing gullies in southern China, Land Use Policy, 32, 119-124, 2013.
715 Zhuang Y. T., Huang Y. H., Lin J. S., Jiang F. S., Zheng Y. and Sun S.X., et al.: Study on liquid limit and plastic
716 limit characteristics and factors of Benggang in red soil layer, Research of Soil and Water Conservation, 21, 208-
717 216, 2014 (in Chinese).
718 Zolfaghari Z., Mosaddeghi M. R., Ayoubi S., and Kelishadi H.: Soil Atterberg limits and consistency indices as
719 influenced by land use and slope position in western Iran, J. Mt. Sci-engl., 12:, 1471-1483, 2015.

720 **Tables**

721 **Table 1.** Description of soil sample site

722 **Table 2.** Description of weathering profile, soil sampling depth and soil properties for different weathering profiles of the four
723 collapsing gullies

724 **Table 3.** Percentages of different particle-size distributions for different weathering profiles of the four collapsing gullies

Solid Earth Discuss., doi:10.5194/se-2016-152, 2016
Manuscript under review for journal Solid Earth
Published: 9 December 2016

725 **Table 4.** Soil Atterberg limits for different weathering profiles of the four collapsing gullies

726 **Table 5.** Regression and correlation analysis of soil Atterberg limits with soil physico-chemical properties

727

728 **Table 1.** Description of soil sample site

Location	Collapsing gully code	Longitude and latitude	Altitude (m)	Height of collapsing gully wall(m)	Coverage of tree layer (%)	Coverage of surface layer (%)	Vegetation community
Tongcheng County	TC	29°12′39″N 113°46′26″E	142	9	45	64	*Pinus massoniana* + *Cunninghamia lanceolata* + *Liquidambar formosana* + *Phyllostachys heterocycla* - *Rosa laevigata* + *Smilax china* + *Gardenia jasminoides* + *Vaccinium carlesii* + *Lespedeza bicolor* - *Dicranopteris linearis* + *Miscanthus floridulus*
Gan County	GX	26°11′22.2″N 115°10′39.4″E	175	15	35	38	*P. massoniana* + *L. formosana* + *Schima superba* - *L. bicolor* - *D. linearis*
Anxi County	AX	24°57′14.3″N 118°3′35.1″E	172	20	30	43	*P. massoniana* + *Eucalyptus robusta* + *Acacia confusa* - *Rhus chinensis* + *Rhodomyrtus tomentosa* + *Loropetalum chinense* - *D. linearis* +*M. floridulus*
Wuhua County	WH	24°06′10.4″N 115°34′57.1″E	157	35	28	35	*P. massoniana* - *R. tomentosa* + *Baeckea frutescens* - *D. linearis*

729

730 **Table 2.** Description of weathering profile, soil sampling depth and soil properties for different weathering profiles of the four

731 collapsing gullies

Soil layer code	Weathering profile	D (m)	PD (g cm^{-3})	BD (g cm^{-3})	TP (%)	SOM (g kg^{-1})	CEC (cmol kg^{-1})	Fed (g kg^{-1})
TC1	Surface layer	0.3	2.58	1.29 ± 0.05d	49.03 ± 2.37a	23.37 ± 0.55a	16.39 ± 0.90a	21.38 ± 0.46bc
TC2	Red soil layer	0.8	2.64	1.47 ± 0.01a	44.11 ± 0.29c	6.81 ± 0.17b	8.37 ± 1.14b	27.37 ± 0.84a
TC3	Red soil layer	2	2.68	1.34 ± 0.05c	49.53 ± 1.79a	5.84 ± 0.20c	7.59 ± 0.27b	23.29 ± 1.29b
TC4	Red soil layer	4	2.65	1.39 ± 0.02b	47.26 ± 0.85b	2.68 ± 0.13d	3.32 ± 0.44c	19.42 ± 1.72c
TC5	Sandy soil layer	7	2.62	1.33 ± 0.02c	49.72 ± 0.83a	1.20 ± 0.11e	4.07 ± 0.61c	13.84 ± 0.93d
TC6	Sandy soil layer	9	2.65	1.35 ± 0.01c	48.63 ± 0.35ab	1.02 ± 0.06e	3.92 ± 0.34c	11.89 ± 1.00e
GX1	Surface layer	0.3	2.57	1.27 ± 0.05c	50.94 ± 2.34a	7.93 ± 0.11a	10.28 ± 0.17a	25.31 ± 1.45a
GX2	Red soil layer	0.8	2.67	1.40 ± 0.03ab	47.65 ± 1.50b	1.35 ± 0.08b	8.27 ± 0.44bc	26.59 ± 2.90a
GX3	Red soil layer	1.8	2.64	1.40 ± 0.02ab	46.79 ± 0.87bc	1.07 ± 0.12c	7.91 ± 0.60c	22.72 ± 0.57bc
GX4	Red soil layer	4	2.63	1.42 ± 0.02a	46.02 ± 0.95c	0.86 ± 0.07d	8.90 ± 0.69b	23.96 ± 1.11b
GX5	Sandy soil layer	7.5	2.62	1.41 ± 0.02ab	46.13 ± 1.06c	0.42 ± 0.06f	5.41 ± 0.86d	18.36 ± 0.77c
GX6	Sandy soil layer	9	2.69	1.37 ± 0.04bc	49.20 ± 1.59ab	0.72 ± 0.09e	5.98 ± 0.52d	13.30 ± 0.43d
GX7	Detritus layer	11	2.64	1.33 ± 0.06c	48.32 ± 1.27b	0.40 ± 0.06f	2.09 ± 0.19e	9.90 ± 0.78e
GX8	Detritus layer	13.5	2.59	1.38 ± 0.04ab	46.65 ± 1.96bc	0.71 ± 0.11e	3.43 ± 0.36e	9.41 ± 0.63e
AX1	Surface layer	0.3	2.54	1.31 ± 0.06c	44.40 ± 2.78d	44.06 ± 0.04a	22.18 ± 0.21a	31.03 ± 1.80a

Solid Earth Discuss., doi:10.5194/se-2016-152, 2016
Manuscript under review for journal Solid Earth
Published: 9 December 2016

AX2	Red soil layer	0.8	2.63	1.39 ±0.06ab	54.24±2.89a	11.23 ±0.61b	14.63±1.30b	27.53±0.56b
AX3	Red soil layer	2	2.66	1.43 ±0.03a	52.38±1.73ab	6.33 ±0.11c	9.20±0.58c	26.35±0.74b
AX4	Red soil layer	4	2.60	1.41 ±0.01a	50.81±0.45b	2.41 ±0.11d	6.37±0.61d	24.38±1.11c
AX5	Sandy soil layer	8	2.65	1.37 ±0.03b	48.39±1.31bc	0.82 ±0.03f	4.82±0.18e	11.87±1.04d
AX6	Sandy soil layer	10	2.54	1.35 ±0.02bc	47.01±0.88c	1.31 ±0.09e	5.02±0.27de	10.55±1.23d
AX7	Detritus layer	12	2.62	1.32 ±0.02c	49.50±0.82bc	0.81 ±0.07f	2.36±0.32f	7.34±0.56e
AX8	Detritus layer	15	2.53	1.31 ±0.02c	48.12±1.33bc	0.67 ±0.09f	3.80±0.71ef	7.30±0.80e
WH1	Surface layer	0.3	2.52	1.33 ±0.04d	48.19±0.93a	15.17 ±1.73a	13.84±0.88a	28.40±0.64a
WH2	Red soil layer	1	2.69	1.48 ±0.01b	44.96±0.29c	4.65 ±0.29b	7.69±0.39b	24.52±0.54b
WH3	Red soil layer	2.5	2.72	1.47 ±0.03b	45.68±1.15bc	2.59 ±0.14c	6.62±0.51b	22.94±0.91bc
WH4	Sandy soil layer	5	2.68	1.44 ±0.02c	46.15±0.83b	2.82 ±0.03c	6.54±0.45b	16.28±1.10c
WH5	Sandy soil layer	9	2.63	1.40 ±0.03cd	46.44±1.64b	1.61 ±0.10d	4.18±0.50c	12.41±0.27d
WH6	Sandy soil layer	11	2.62	1.49 ±0.02b	43.01±1.01c	0.57 ±0.08f	2.28±0.22d	14.23±0.78cd
WH7	Detritus layer	14	2.59	1.54 ±0.03a	40.34±1.46d	0.74 ±0.05e	3.91±0.18cd	8.86±0.40e
WH8	Detritus layer	17	2.61	1.37 ±0.05d	46.41±1.59b	0.23 ±0.18g	1.93±0.30e	8.37±0.32e

732 Values with different letters are significantly different at the P < 0.05 level among the different soil layers of the same collapsing

733 gully. SOM: soil organic matter; Fe_d =Free iron oxide

734 **Table 3.** Percentages of different particle-size distributions for different weathering profiles of the four collapsing gullies

Soil layer code	Mass percentages of soil particle-size distribution (mm)									
	Gravel	Coarse sand		Fine sand		Silt				Clay
	2.0-12.0-1.0	1.0-0.5	0.5-0.25	0.25-0.15	0.15-0.05	0.05-0.02	0.02-0.01	0.01-0.005	0.005-0.002	<0.002
TC1	9.24±1.61b	7.13±0.10d	7.09±1.35b	3.97±0.64d	9.86±0.93c	6.55±1.67d	12.07±0.59a	5.16±0.58c	6.11±0.81b	32.81±1.46b
TC2	7.87±0.65b	6.55±0.12e	6.12±0.54c	6.10±0.07c	6.24±0.93d	16.67±1.04a	9.81±0.50b	6.18±1.07b	5.54±0.92c	28.91±0.62c
TC3	4.51±0.36c	4.91±0.24f	5.27±0.11d	6.72±0.85bc	10.55±1.14c	6.34±1.22d	9.74±1.16b	3.66±0.84d	7.26±0.21a	41.03±0.72a
TC4	3.05±0.55d	7.95±0.54c	9.78±1.08a	9.19±1.32a	17.66±1.57a	6.25±0.60d	10.97±0.96a	3.27±0.63d	5.69±0.55c	26.19±1.86d
TC5	5.34±0.71c	11.14±0.38b	11.75±0.78a	10.21±1.05a	13.68±1.45b	14.01±1.16b	9.44±0.17b	7.54±0.25a	6.64±0.79b	10.24±0.18e
TC6	19.84±2.28a	14.63±0.58a	11.95±1.23a	7.58±0.37b	16.46±1.04a	8.28±0.91c	8.48±0.98c	5.20±0.33c	3.71±0.13d	3.87±0.48f
GX1	8.99±0.37d	4.78±0.10d	4.43±0.29e	3.94±0.18e	12.77±0.34f	2.92±0.25e	5.49±0.78d	6.09±1.03e	13.92±1.65a	36.65±1.85a
GX2	8.12±0.31e	4.66±0.19d	4.41±0.05e	4.17±0.22e	13.62±0.31de	4.14±0.66d	7.92±1.27bc	7.00±1.10d	12.85±1.62a	33.10±1.80b
GX3	9.89±0.50c	5.65±0.21c	6.19±0.25d	5.32±0.41d	16.40±1.03c	9.24±0.33c	7.19±1.74c	8.50±0.65a	10.37±0.88b	21.25±1.14c
GX4	8.85±0.71d	5.68±0.30c	7.93±0.31b	8.68±0.53b	18.72±1.27b	8.80±0.45c	8.09±0.21b	7.65±0.48c	9.81±0.41bc	15.78±0.39d
GX5	9.71±1.30cd	5.03±0.25d	4.17±0.39e	4.91±0.42d	27.91±0.96a	11.14±0.54b	8.49±1.4b	6.68±1.43d	7.69±1.25d	14.29±0.55d
GX6	12.13±0.73b	7.90±0.19b	7.30±0.19c	8.69±0.40b	16.40±0.34c	12.44±0.52a	8.62±0.59b	8.24±0.53a	9.37±0.71c	8.90±0.42f
GX7	14.87±1.28a	8.87±0.14a	8.60±0.81ab	9.84±0.99a	14.60±0.72d	10.37±1.63bc	6.03±0.82d	8.83±0.17a	4.44±1.99e	13.55±1.39de
GX8	15.83±0.85a	8.80±0.07a	8.67±0.20a	8.09±0.62c	13.15±0.99ef	11.18±1.11ab	9.73±1.47a	7.68±0.31c	5.31±1.46e	11.55±1.11e
AX1	19.32±0.48c	7.55±0.42c	6.67±0.23c	3.86±0.18d	6.52±0.94d	5.04±0.95d	6.02±0.37d	3.63±0.47e	7.93±0.24c	33.47±1.39b
AX2	6.23±0.35e	5.34±0.16d	4.10±0.31d	2.90±0.23ef	4.42±0.33e	3.47±0.71e	4.01±0.19e	6.34±1.12c	11.53±1.90ab	51.66±1.54a

Solid Earth Discuss., doi:10.5194/se-2016-152, 2016
Manuscript under review for journal Solid Earth
Published: 9 December 2016

AX3	6.39±0.25e	5.66±0.21d	3.99±0.43d	3.21±0.13e	6.42±1.02d	4.19±0.97de	1.60±0.62f	5.64±1.35cd	9.61±0.69b	53.27±1.47a
AX4	8.65±0.74d	4.63±0.08e	3.31±0.16e	2.48±0.50f	12.22±1.02c	3.92±1.81e	8.27±1.17ab	11.65±0.56a	12.91±1.91a	31.96±0.55b
AX5	19.86±0.87bc	8.71±0.23b	6.08±0.29c	5.35±0.12c	14.30±1.81bc	8.62±0.48c	8.02±1.53b	8.35±0.37b	4.04±1.32d	16.68±1.10c
AX6	24.49±1.05a	10.01±0.42a	7.66±0.45b	6.44±1.02ab	15.82±1.44ab	10.71±0.50b	6.87±1.11cd	6.58±1.13c	4.27±0.07d	7.14±1.33d
AX7	19.15±0.35c	7.83±0.27c	7.04±0.57b	5.95±0.69b	15.96±0.78a	15.85±1.12a	8.00±0.74bc	8.00±0.48b	3.78±0.73d	8.45±0.31d
AX8	21.02±1.37b	10.93±0.43a	10.86±0.98a	7.94±1.76a	17.48±1.97a	8.73±1.08c	9.00±0.30a	5.01±0.27d	1.02±0.49e	8.00±1.25d
WH1	18.53±0.62f	5.67±0.12c	3.74±0.17c	2.30±0.39d	10.24±1.15a	9.33±1.30a	5.55±0.19d	4.59±0.62d	7.42±1.85d	32.62±1.30a
WH2	23.42±0.40d	5.78±0.09c	2.93±0.21de	2.29±0.05d	6.89±0.74c	7.34±0.56c	8.51±1.28a	3.70±0.55d	10.23±1.32c	28.92±2.22b
WH3	25.72±1.91b	5.92±0.29c	2.76±0.08e	1.97±0.05d	5.15±0.18d	5.74±0.53d	4.29±0.63e	8.72±0.93c	12.91±0.15b	26.83±1.82b
WH4	22.26±1.33de	6.39±0.21b	3.24±0.25d	2.06±0.10d	4.96±1.10d	5.45±1.25d	7.09±1.00bc	9.10±0.60c	16.07±1.60a	23.38±1.97c
WH5	24.53±0.62c	8.46±0.16a	4.29±0.27b	3.05±0.14c	5.67±1.34d	7.02±0.76c	4.04±0.94e	15.15±1.85a	10.23±1.03c	17.54±1.67d
WH6	27.73±0.23a	8.50±0.41a	5.00±0.49a	4.40±0.37b	3.06±0.38e	10.94±1.25a	6.98±1.34bc	12.39±0.65b	10.06±1.73c	10.93±1.38e
WH7	25.81±0.25b	8.54±0.05a	5.29±0.29a	5.57±0.24a	9.27±0.86ab	8.36±1.80ab	6.73±0.73c	14.46±1.25ab	5.56±0.38d	10.42±0.79e
WH8	25.16±0.82b	8.48±0.17a	5.42±0.08a	5.24±0.61a	8.43±0.49b	7.40±1.66bc	7.55±1.80ab	15.65±1.21a	10.91±0.57c	5.77±0.82f

735 Values with different letters are significantly different at the $P < 0.05$ level among the different soil layers of the same collapsing

736 gully.

737

738 **Table 4.** Soil Atterberg limits for different weathering profiles of the four collapsing gullies

Soil layer code	Plastic limit (%)	Liquid limit (%)	Plasticity index (%)	Liquidity index (%)
TC1	35.93±0.69a	62.68±1.32a	26.75±2.01a	-49.55±3.74d
TC2	31.73±2.25b	53.09±0.20bc	21.36±2.05b	-47.08±4.52d
TC3	30.51±0.72b	56.03±2.20b	25.52±1.47a	-27.60±1.59b
TC4	31.74±0.56b	50.04±0.23c	18.30±0.33c	-35.54±6.96c
TC5	20.73±1.68c	35.31±1.05d	14.58±2.73d	-37.25±6.96c
TC6	19.43±2.07c	30.91±0.25d	11.48±1.82d	-10.57±1.68a
GX1	33.82±0.13a	57.70±2.16a	23.88±2.04ab	-50.36±4.29e
GX2	27.04±2.81b	52.91±0.61b	25.87±2.20a	-34.67±2.94d
GX3	23.08±0.45c	49.58±0.96bc	26.50±1.41a	-30.54±1.62c
GX4	23.97±2.39c	45.82±3.61c	21.85±1.22b	-25.80±1.44bc
GX5	22.88±1.98cd	43.32±1.45c	20.44±0.53b	-24.27±0.63bc
GX6	19.51±0.95d	30.89±2.02e	11.38±1.07d	-22.42±2.10b
GX7	21.16±1.53cd	34.25±0.41d	13.09±1.12c	-18.16±1.57a
GX8	22.06±0.59cd	32.15±1.44de	10.09±2.03d	-17.61±3.56a
AX1	35.58±1.70a	65.71±0.02a	30.14±1.72a	-64.57±3.70d
AX2	36.03±2.83a	60.67±0.11ab	24.64±2.72b	-52.16±5.76c
AX3	35.42±0.21a	57.01±4.56b	21.59±4.36bc	-52.00±10.49c
AX4	25.84±1.60b	48.34±0.71c	22.49±2.31bc	-26.59±2.73b

Solid Earth Discuss., doi:10.5194/se-2016-152, 2016
Manuscript under review for journal Solid Earth
Published: 9 December 2016

AX5	22.34±1.65bc	40.66±0.12cd	18.32±1.53c	-24.12±2.00b
AX6	19.51±0.44d	32.51±1.18e	13.00±0.74d	-24.27±1.40b
AX7	19.32±0.31d	36.26±0.98d	16.94±0.68cd	-13.35±0.54a
AX8	20.95±1.36c	32.48±1.36e	11.53±0.02e	-12.41±0.01a
WH1	36.56±0.99a	62.70±1.04a	26.14±0.05a	-65.91±0.13e
WH2	26.01±2.36b	52.20±0.97b	26.19±3.32a	-31.84±4.03b
WH3	24.93±0.17bc	46.86±2.09c	21.93±1.92b	-42.67±3.74d
WH4	23.83±0.10c	46.11±0.86c	22.28±0.96b	-38.60±1.68bcd
WH5	22.25±0.62c	39.11±0.29d	16.87±0.33c	-36.69±0.70bc
WH6	19.74±0.84d	34.22±1.95e	14.48±1.11cd	-13.38±1.00a
WH7	19.56±0.27d	30.77±1.32f	11.21±1.59d	-11.65±1.63a
WH8	18.91±1.44d	31.72±0.48f	12.81±1.93d	-12.24±1.85a

Table 5. Regression and correlation analysis of soil Atterberg limits with soil physico-chemical properties

	Plastic limit		Liquid limit	
	Regression equations	R^2	Regression equations	R^2
Gravel content	y = -5.083ln(x) + 38.722	0.255	y = -8.323ln(x) + 66.423	0.202
Coarse sand content	y = -8.895ln(x) + 48.448	0.214	y = -21.66ln(x) + 100.51	0.374
Fine sand content	y = -4.772ln(x) + 38.804	0.131	y = -9.633ln(x) + 71.562	0.158
Sand content	y = -17.16ln(x) + 90.809	0.580	y = -32.52ln(x) + 168.51	0.616
Silt content	y = -19.2ln(x) + 91.772	0.320	y = -28.59ln(x) + 143.51	0.210
Clay content	y = 7.6773ln(x) + 3.4506	0.736	y = 14.915ln(x) + 1.8834	0.820
BD	y = -28.04ln(x) + 34.789	0.044	y = -35.65ln(x) + 56.651	0.021
PD	y = -49.17ln(x) + 73.088	0.023	y = -27.35ln(x) + 71.436	0.002
TP	y = 35.364ln(x) - 110.82	0.117	y = 51.702ln(x) - 154.49	0.074
SOM	y = 4.2553ln(x) + 22.753	0.816	y = 7.6856ln(x) + 39.781	0.785
CEC	y = 7.9009ln(x) + 11.719	0.636	y = 15.682ln(x) + 17.359	0.739
Fe_d	y = 10.629ln(x) - 4.226	0.630	y = 21.885ln(x) - 16.509	0.788

Figure Captions

Figure 1. A typical collapsing gully in the hilly granitic region, Anxi County, Fujian Province

Figure 2. Average of soil properties for different weathering profiles of the four collapsing gullies.

Figure 3. Average of different particle-size distributions for different weathering profiles of the four collapsing gullies.

Figure 4. Average of soil Atterberg limits for different weathering profiles of the four collapsing gullies.

Figure 5. Relationship between soil Atterberg limits and soil depth.

Solid Earth Discuss., doi:10.5194/se-2016-152, 2016
Manuscript under review for journal Solid Earth
Published: 9 December 2016

748 **Figure 6.** Correlations between soil Atterberg limits and soil physico-chemical properties.

749

750 **Figure 1.** A typical collapsing gully in the hilly granitic region, Anxi County, Fujian Province (photo: Shuwen Ding)

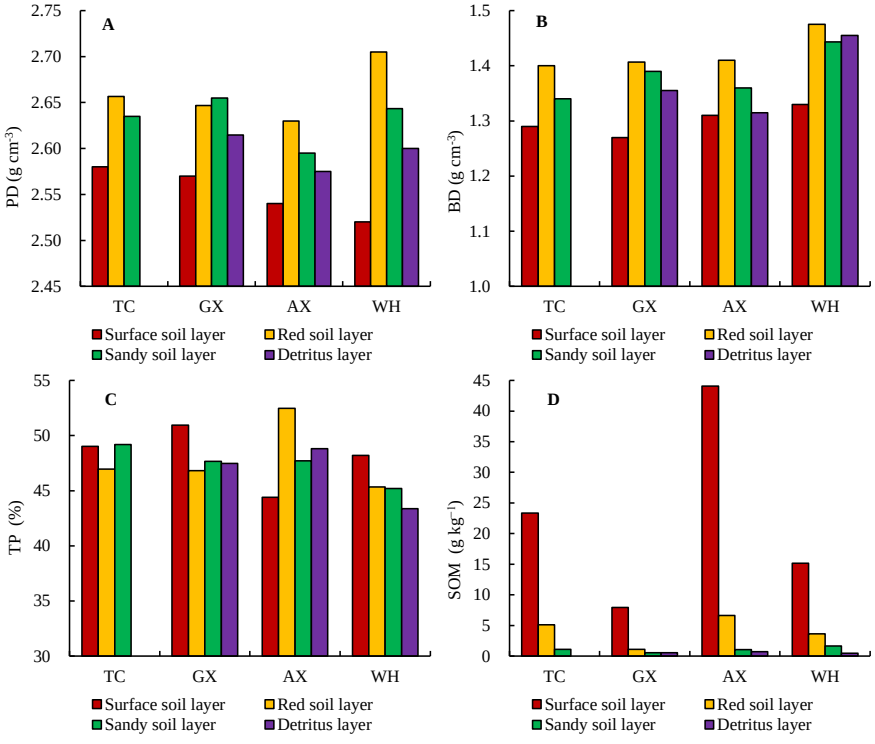

751

752

Solid Earth Discuss., doi:10.5194/se-2016-152, 2016
Manuscript under review for journal Solid Earth
Published: 9 December 2016

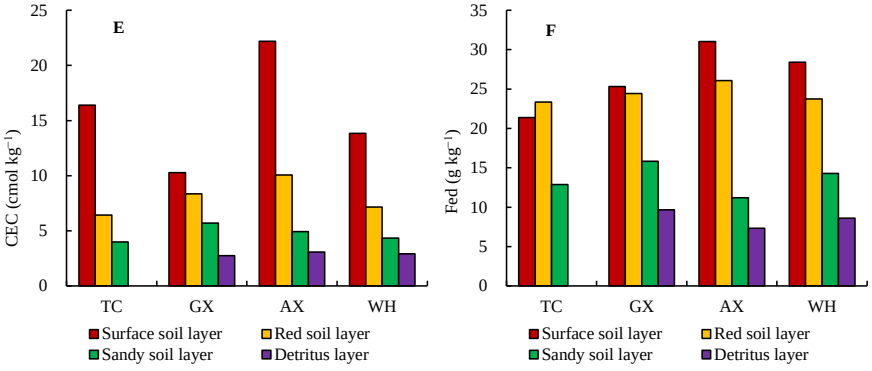

Figure 2. Average of soil properties for different weathering profiles of the four collapsing gullies. (A) particle density; (B) bulk density; (C) total porosity; (D) soil organic matter; (E) cation exchange capacity; and (F) Free iron oxide.

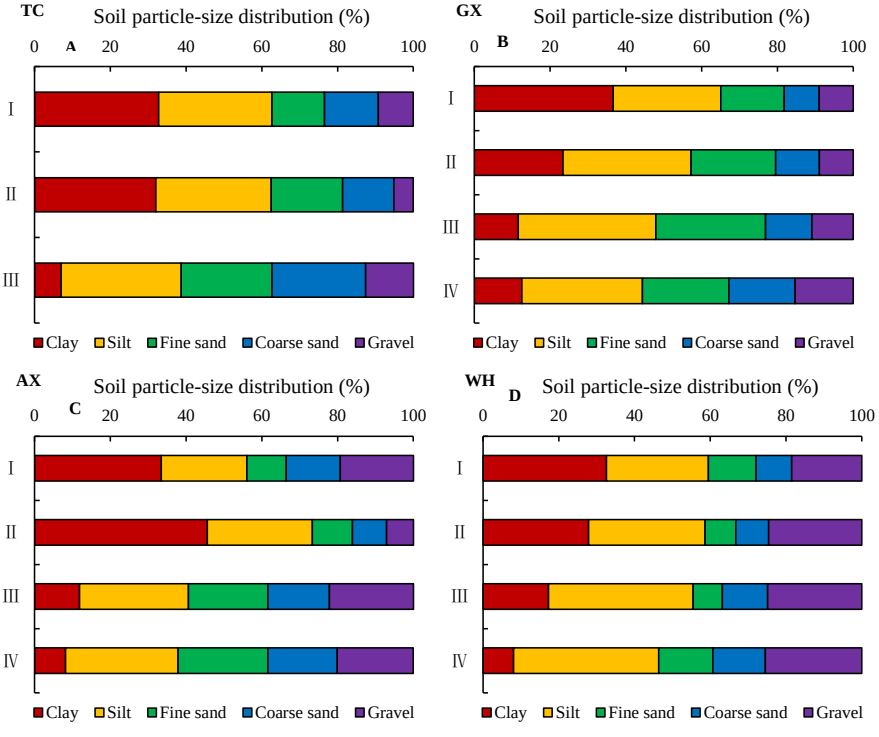

Ⅰ: Surface soil layer; Ⅱ: Red soil layer; Ⅲ: Sandy soil layer; Ⅳ: Detritus layer

Figure 3. Average of different particle-size distributions for different weathering profiles of the four collapsing gullies. (A) Tongcheng county; (B) Ganxian county; (C) Anxi county; and (D) Wuhua county.

Solid Earth Discuss., doi:10.5194/se-2016-152, 2016
Manuscript under review for journal Solid Earth
Published: 9 December 2016

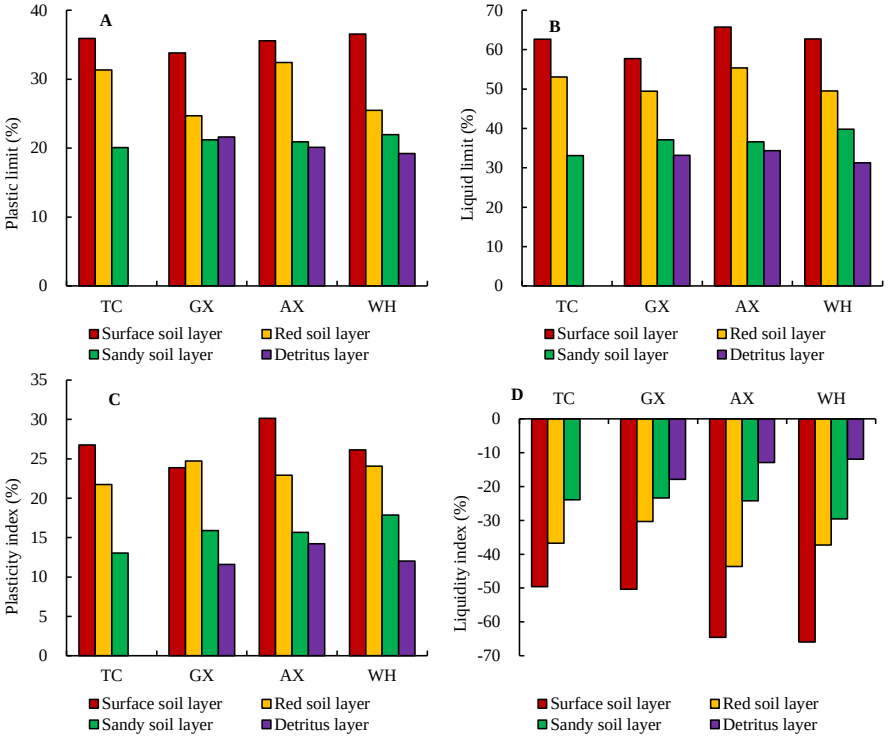

761

762

763 **Figure 4.** Average of soil Atterberg limits for different weathering profiles of the four collapsing gullies. (A) plastic limit; (B)

764 liquid limit; (C) plasticity index; and (D) liquidity index.

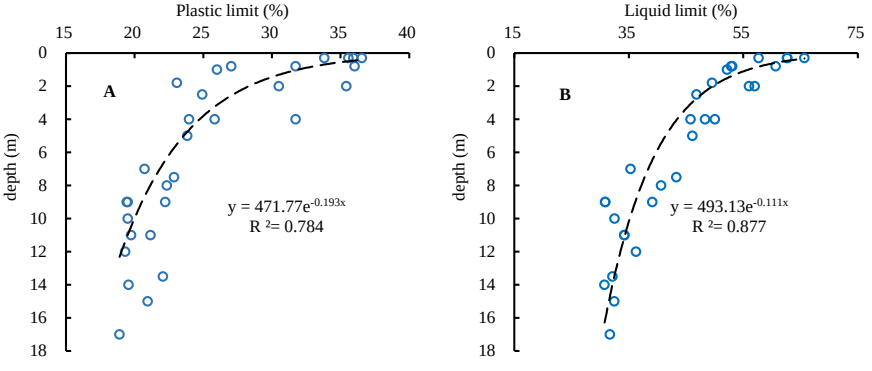

765

Solid Earth Discuss., doi:10.5194/se-2016-152, 2016
Manuscript under review for journal Solid Earth
Published: 9 December 2016

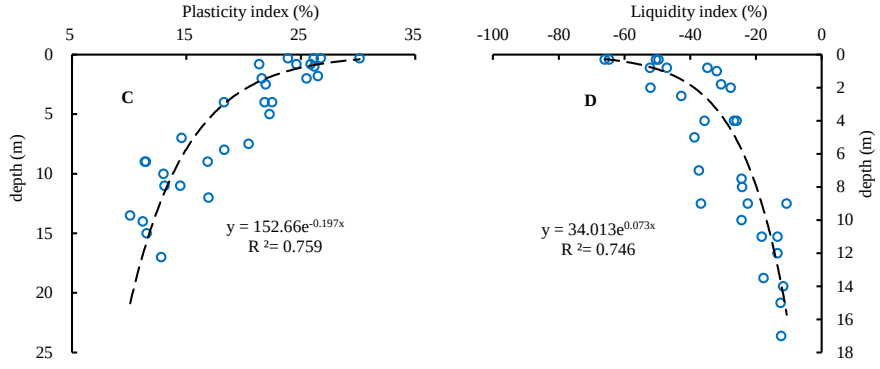

766

767 **Figure 5.** Relationship between soil Atterberg limits and soil depth. (A) plastic limit; (B) liquid limit; (C) plasticity index; and (D)

768 liquidity index.

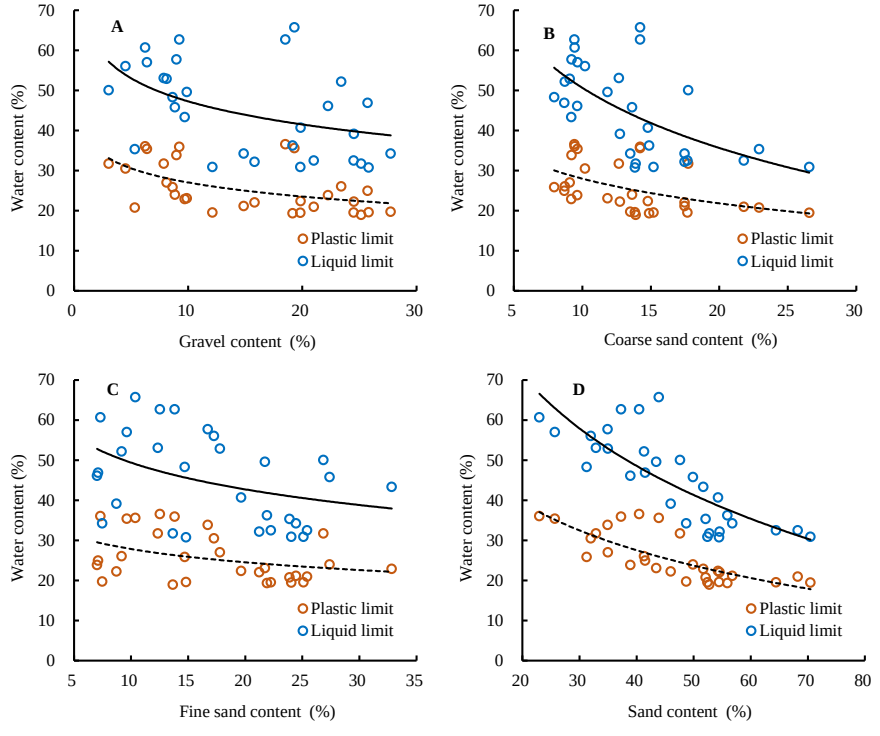

769

770

Solid Earth Discuss., doi:10.5194/se-2016-152, 2016
Manuscript under review for journal Solid Earth
Published: 9 December 2016

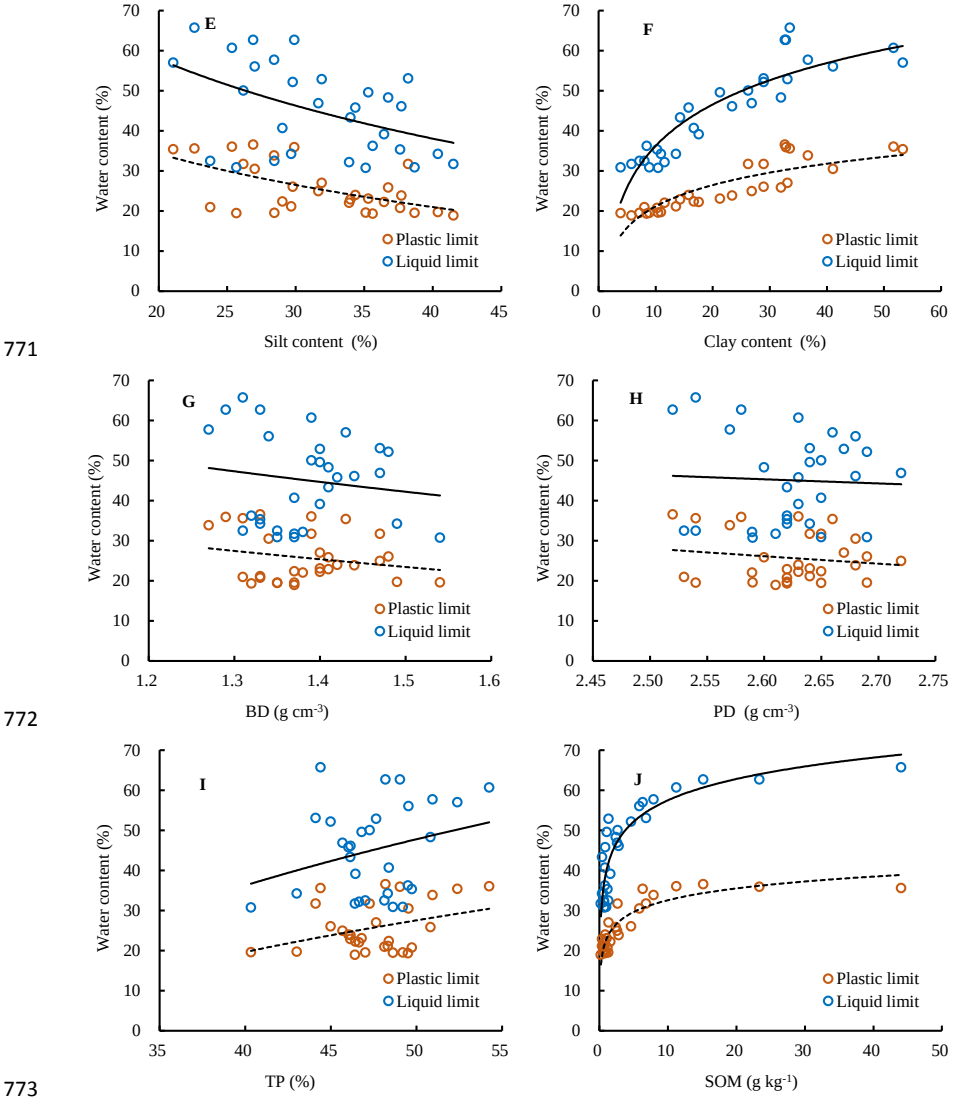

771

772

773

Solid Earth Discuss., doi:10.5194/se-2016-152, 2016
Manuscript under review for journal Solid Earth
Published: 9 December 2016

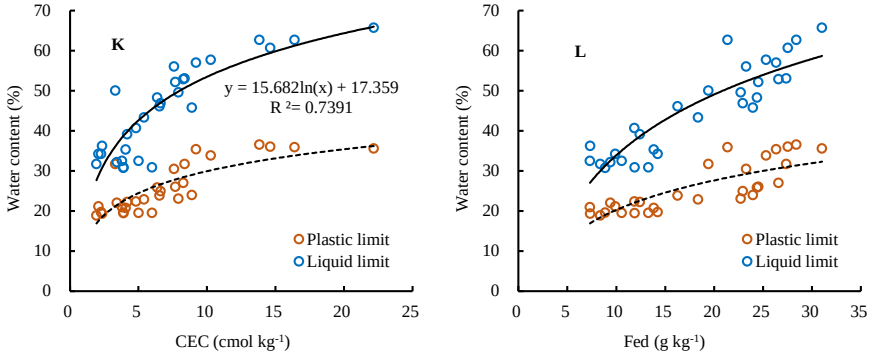

774

775 **Figure 6.** Correlations between soil Atterberg limits and soil physico-chemical properties. (A) gravel content; (B) Coarse sand

776 content; (C) fine sand content; (D) sand content; (E) silt content; (F) clay content; (G) bulk density; (H) particle density; (I) total

777 porosity; (J) soil organic matter; (K) cation exchange capacity; and (L) Free iron oxide.

778